Analytical Methods

Accepted Manuscript

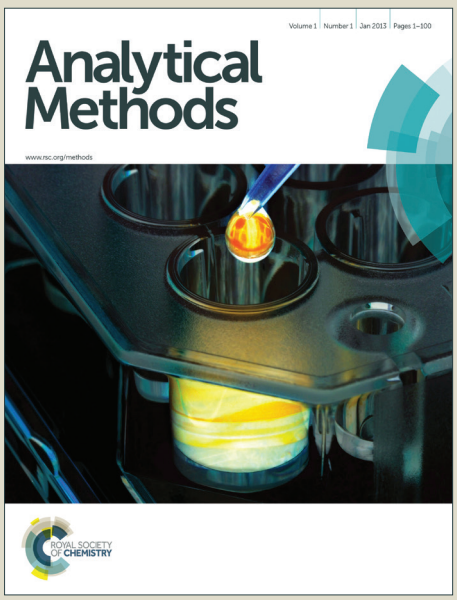

ROYAL SOCIETY OF CHEMISTRY

www.rsc.org/methods

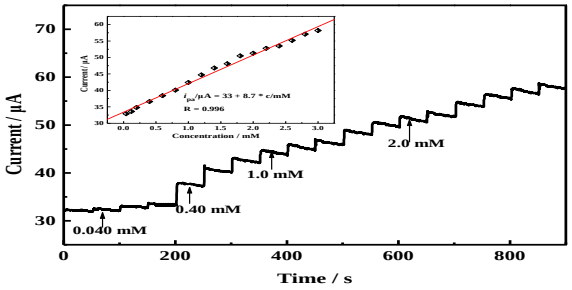

Current-time plot of glucose with increasing concentrations on Cu_2O-attapulgite/RGO/GCE in 0.10 M NaOH solution

Analytical Methods

Full Research Articles

Novel one-pot hydrothermal fabrication of cuprous oxide-attapulgite/graphene for non-enzyme glucose sensing

Susu Zhang,[a] Guangli, Zhang,[a] Ping He,[*a] Wen Lei,[a] Faqin Dong,[a] Dingming Yang,[a] and Zhirong Suo[b]

Received (in XXX, XXX) Xth XXXXXXXXX 20XX, Accepted Xth XXXXXXXXX 20XX

DOI: 10.1039/b000000x

A novel cuprous oxide-attapulgite/graphene based non-enzyme biosensor was constructed successfully for the detection of glucose. Graphite oxide and Cu^{2+}-functionalized attapulgite were simultaneously reduced by hydrazine hydrate under mild hydrothermal conditions in one pot, and subsequently dried at 80 ℃ in air to obtain cuprous oxide-attapulgite/graphene composites. The composites were characterized by XRD, Raman spectra, EDX and SEM. Due to the synergistic effect of cuprous oxide-attapulgite and graphene, as prepared composites presented excellent electrocatalytic performances. The cuprous oxide-attapulgite/graphene modified electrode exhibited sensitive linear amperometric responses to glucose in concentration range of 4.0 $\times 10^{-5}$ M ~ 3.0 $\times 10^{-3}$ M (R = 0.996), and the detection limit was calculated as 2.1 $\times 10^{-6}$ M. The as prepared modified electrode was highly selective to glucose in the presence of common interfering species in biological fluids, such as dopamine, ascorbic acid and uric acid.

1 Introduction

As a common chronic disease, hyperglycemia usually occurs when glucose concentration exceeds the normal range of 80 ~ 120 mg/dL (4.4 ~ 6.6 mM), which may result in metabolic and systematic disorder[1]. Therefore, some efforts have been made to developing various methods for monitoring glucose for diagnosis of diabetes, such as optical techniques, capacitive detections, coulometric measurements and amperometric methods[2-4]. Particularly, the development of amperometric sensors for the detection of glucose has attracted extensive attention due to its high sensitivity, high reliability, fast response, good selectivity and low cost[5]. It should be noted that most of amperometric glucose biosensors are usually based on glucose oxidase enzymes (GOx) due to its high sensitivity and selectivity to glucose. However, natural enzymes are not only expensive but also unstable on account of the intrinsic nature of enzymes[6]. Therefore, considerable attention has been paid to the development of non-enzyme glucose biosensors to deal with these disadvantageous limitations. Up to now, some modified electrodes, such as Ni hydroxide modified nitrogen-incorporated nanodiamonds modified electrode[7], AuNP–ATP–cMWCNT coated glassy carbon electrode (GCE)[8] and Ni nanowire modified electrode[9], have been reported for the detection of glucose, offering a potential possibility for the applications in clinical use.

In the effort to decrease the cost of sensors fabricated with noble metals, it is necessary to develop highly sensitive, reliable and low-cost biosensors with excellent electrocatalytic activity for the oxidation of glucose. Nowadays, owing to their high catalysis, low cost and good stability, metal oxide nanomaterials are widely used in fabricating modified electrodes. Cuprous oxide (Cu_2O) is an important p-type semiconductor with wide potential applications in many fields such as conversion of solar energy[10], lithium ion batteries[11], electrocatalysis[12] and gas sensors[13]. A variety of methods including electrochemical deposition, hydrothermal process and solution phase growth have been developed for the preparation of Cu_2O nanomaterials[14,15]. Notably, individual Cu_2O nanoparticles are vulnerable to form agglomerations during preparation procedure because of the high surface energy and strong interaction forces between nanoparticles[16]. Therefore, developing a convenient approach to prepare well-dispersed Cu_2O based nanocomposites is of realistic significance.

Attapulgite, a kind of natural nanostructured clay, is a crystalline hydrated magnesium aluminum silicate with fibrous morphology. The zeolite-like channels of mineral result in high adsorption and penetrability due to its regular structure and large specific surface area. In this sense, attapulgite has attracted increasing attention and been widely employed in different fields such as adsorption[17], hydrogen storage[18] and cyclohexene hydrogenation[19]. To the best of our knowledge, attapulgite is also expected to be applied as the support for size-selected nanoparticles to obtain functional materials in the form of nano-dispersion, making active sites more readily accessible[20].

Recently, reduced graphite oxide (RGO) has attracted tremendous attentions and thus inherits numerous applications in nanomaterials and nanotechnology because of its unique electronic, optical and chemical properties[21]. RGO, with two-dimensional plane, provides itself with excellent conductivity and large specific surface area for the immobilization substances including a wide range of nanoparticles and biomolecules, etc[22,23]. However, it is worth noting that the agglomeration of RGO is an essential problem to be addressed in order to prevent the formation of agglomerates and allow the fast diffusion of target molecules.

In our work, by taking advantages of large surface area and high electronic conductivity of RGO and high electrocatalytic activity of Cu_2O-attapulgite, we presented a novel Cu_2O-attapulgite/RGO modified GCE for the detection of glucose. Firstly, the presence of attapulgite could largely reduce the size of Cu_2O nanoparticles

and prevent the nanoparticles from aggregating. Secondly, RGO was beneficial to effectively improve electrochemical stability of Cu_2O-attapulgite nanoparticles. Thirdly, due to the high electro-conductivity of RGO, Cu_2O-attapulgite/RGO hybrids presented improved electron transfer ability. The integration of different ingredients combined merits of each component and yielded enhanced properties via synergistic effect. As prepared Cu_2O-attapulgite/RGO modified electrode exhibited linear amperometric responses towards glucose in the concentration range of 4.0×10^{-5} M ~ 3.0×10^{-3} M (R = 0.996) and the detection limit was down to 2.1×10^{-6} M.

2 Experimental

2.1 Chemicals and reagents

Graphite powder was purchased from Sigma-Aldrich. $CuSO_4 5H_2O$, NaOH, $N_2H_4\ H_2O$ and $HCON(CH_3)_2$ (DMF) were all analytical grade and purchased from Chengdu Chemical Reagent Co., Ltd. Glucose, dopamine (DA), ascorbic acid (AA) and uric acid (UA) were purchased from Alfa Aesar.

Attapulgite clay was obtained from Mingguang Attapulgite Mine Factory (Anhui, China). Doubly distilled water was used throughout the whole experiments.

2.2 Preparation and characterization of electrode materials

To obtain Cu^{2+} functionalized attapulgite (Cu^{2+}-attapulgite), 100.0 mg attapulgite was dispersed into 100.0 mL 0.020 M $CuSO_4$ solution and kept continuous stirring for 24 h. Subsequently, as prepared Cu^{2+}-attapulgite was separated by filtration and thoroughly washed with distilled water to remove the unbound matter. Finally, the washed precipitate was dried at 60 ℃ for 12 h. Graphite oxide (GO) was synthesized by Hummers method with some modifications[24].

The procedure for preparation of attapulgite-Cu_2O/RGO was described as follows (Scheme 1). Firstly, 50.0 mg Cu^{2+}-attapulgite and 50.0 mg GO were dispersed into 20.0 mL water to form a homogenous mixture by sonication. Subsequently, GO and Cu^{2+}-attapulgite were simultaneously reduced by adding 3.0 mL $N_2H_4\ H_2O$ and the solution was kept reaction at 120 ℃ for 8 h in a teflon-lined stainless steel autoclave with 50.0 mL max-capacity. Finally, the black powder of Cu-attapulgite/RGO was obtained and then was dried at 80 ℃ in air for 48 h until the pale blue colored Cu_2O-attapulgite/RGO was formed by air oxidation. For comparison, attapulgite-Cu_2O and Cu_2O-RGO were prepared according to the similar procedure above just using Cu^{2+}-attapulgite and/or Cu^{2+}-GO as precursor instead of Cu^{2+}-attapulgite/GO.

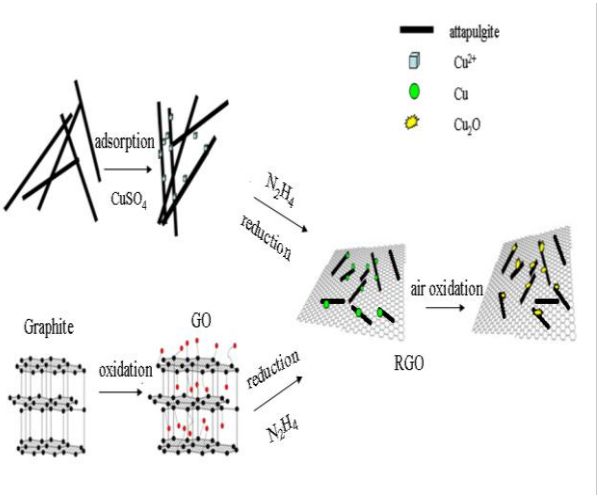

Scheme 1 Formation mechanism of Cu_2O-attapulgite/RGO nanocomposites.

The crystal structures of GO and RGO were characterized by Raman spectrometer (INVIA, England) in wavenumber range of 400 ~ 4000 cm^{-1}. The crystal structures of GO, RGO, attapulgite, Cu_2O-attapulgite and Cu_2O-attapulgite/RGO were characterized by X-ray diffraction analyzer (XRD, X' Pert PRO, PANalytical BV) with Cu K_α radiation (λ = 0.154060 nm) and recorded from 3.0◦ to 80◦ at a speed of 2.0◦ per minute. The morphologies and compositions of attapulgite, Cu_2O-attapulgite, RGO and Cu_2O-attapulgite/RGO were obtained using a scanning electron microscopy connected with Energy Dispersive X-ray analyzer (SEM-EDX, Ultra 55, Zesis).

2.3 Electrode preparation and electrochemical measurements

Prior to use, GCE was successively polished up to a mirror finish with 0.50 μm and 50 nm alumina powders and then washed by sonication in doubly distilled water repeatedly.

5.0 mg Cu_2O-attapulgite/RGO was dispersed into 1.0 mL DMF to form a homogenous mixture by sonication. Cu_2O-attapulgite/RGO/GCE was prepared by casting 5.0 μL attapulgite/Cu_2O/RGO suspension onto GCE and then was dried in air. For comparison, the preparation procedures of Cu_2O-attapulgite/GCE, Cu_2O-RGO/GCE and RGO/GCE were similar to that of Cu_2O-attapulgite/RGO/GCE just replacing Cu_2O-attapulgite/RGO suspension with Cu_2O-attapulgite, Cu_2O-RGO and/or RGO suspension.

The data of cyclic voltammetry (CV) and chronoamperometry (CA) were recorded with PARSTAT 2273 electrochemical workstation (Princeton Applied Research, USA) by introducing a three-electrode test system using platinum electrode as counter electrode, bare or modified GCE as working electrode referred to saturated calomel electrode (SCE).

3 Results and discussion

3.1 Raman spectral characterization

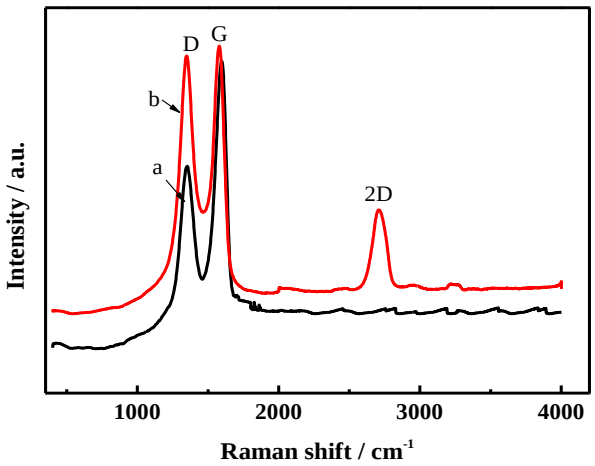

Fig. 1 Raman spectra of GO (a) and RGO (b).

Raman spectrum was a nondestructive tool to characterize carbonaceous materials. As shown in Fig. 1, Raman spectra of both GO and RGO showed D-band at 1350 cm^{-1} ascribed to the breathing mode of k-point phonons of A_{1g} symmetry and G-band at 1580 cm^{-1} corresponding to the first-order scattering of E_{2g}, respectively[25]. The intensity ratio of D and G bands, I_D/I_G, usually indicated a disorder degree and was proportional to the degree of structural defects[26]. It was manifested that I_D/I_G value was calculated as 0.74 for GO (Fig. 1a), while after reduction I_D/I_G value increased to 1.09 for RGO (Fig. 1b). Results obtained in this study agreed well with former researches, indicating that GO was well deoxygenated to RGO. Furthermore, the appearance of a single band of 2D band for RGO was evidence of the presence of a monolayer of RGO[27].

3.2 XRD characterization

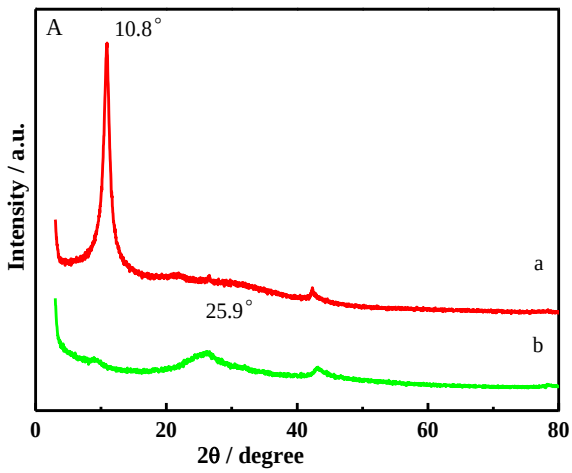

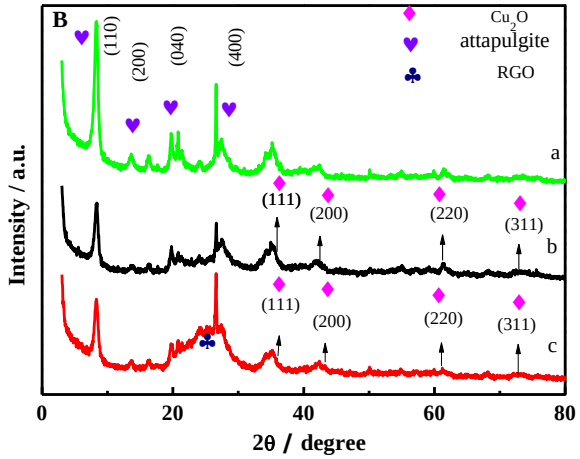

Fig. 2 (A) XRD patterns of GO (a) and RGO (b). (B) XRD patterns of attapulgite (a), Cu_2O-attapulgite (b) and Cu_2O-attapulgite/RGO (c).

Shown in Fig. 2A were XRD patterns of GO and RGO. Compared with Fig. 2A-a, there was no characteristic peak of GO ($2\theta = 10.8°$) or graphite ($2\theta = 24.5°$) in Fig. 2A-b, suggesting that GO was well reduced, and the restacking of the as-reduced graphene sheets was effectively prevented, which was consistent with the results of Raman above. Shown in Fig. 2B were XRD patterns of attapulgite, Cu_2O-attapulgite and Cu_2O-attapulgite/RGO, respectively. The peaks of attapulgite at 8.0, 13.6, 19.7 and 26.6 ° corresponded to the primary diffraction of (110), (200), (040) and (400) planes (Fig. 2B-a)[28]. The XRD pattern of Cu_2O-attapulgite showed no significant difference to that of pure attapulgite, except that the peaks shifted slightly and the intensity became smaller. For Cu_2O-attapulgite, the peaks at 36.5, 42.3, 61.6 and 73.7 ° were attributed to (111), (200), (220) and (311) planes of Cu_2O, where these diffraction signals could not cover up those of attapulgite due to the relatively low weight content of Cu_2O in the composite as well as the shielding effect of attapulgite (Fig. 2B-b). It was known that if the small particles of metal or metal oxides were highly dispersed in the channels of attapulgite, the corresponding diffraction peaks would nearly disappear due to the shielding effects of surrounding hosts[29,30]. With the same preparation scheme, the peaks of Cu_2O-attapulgite/RGO were almost the same as Cu_2O-attapulgite, while there was a broad peak from 20 to 28 ° attributed to the diffraction of RGO, indicating that Cu_2O-attapulgite had been successfully fabricated on RGO (Fig. 2B-c)[31].

3.3 SEM characterization

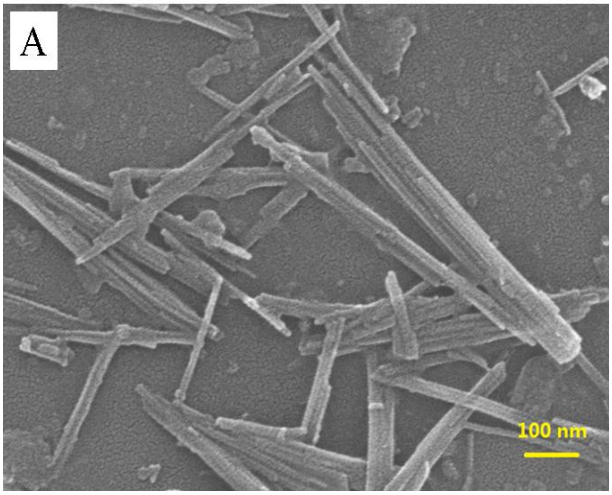

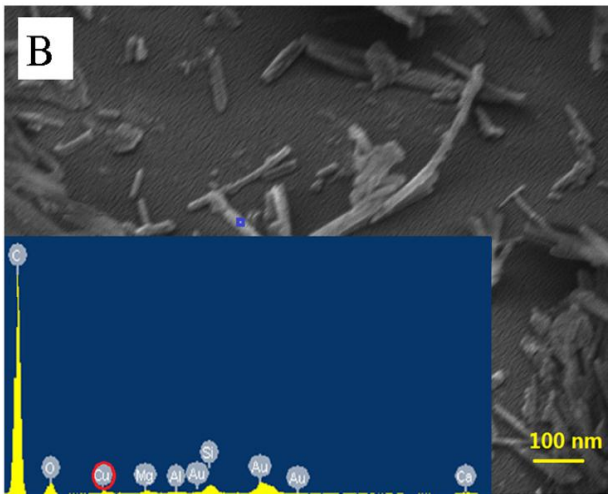

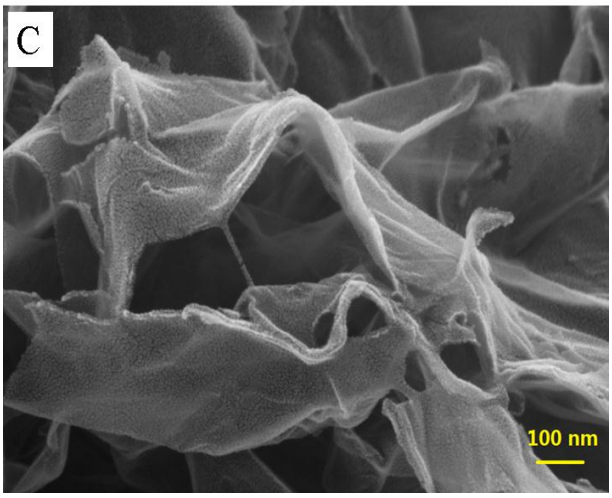

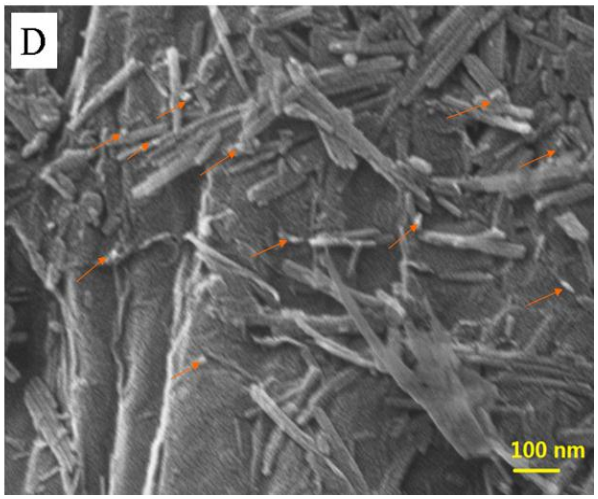

Fig. 3 SEM images of attapulgite (A), Cu_2O-attapulgite (B), RGO (C) and Cu_2O-attapulgite/RGO (D).

Shown in Fig. 3 were SEM images of attapulgite, Cu_2O-attapulgite, RGO and Cu_2O-attapulgite/RGO, respectively. It was found that attapulgite was of average diameter of about 60 ~ 130 nm with morphology of crystal fibers (Fig. 3A). Under hydrothermal conditions, attapulgite was broken into smaller fragments, and small amount of nanoparticles were dispersed on attapulgite. EDX spectrum also showed that small amount of Cu element was doped into attapulgite (Fig. 3B). On the other hand, RGO was crumpled to a curly and wavy shape and interacted with each other to form an open pore system, which allowed electrons to easily access the surface of modified electrodes (Fig. 3C). As for Cu_2O-attapulgite/RGO, there were also small amount of Cu_2O nanoparticles decorating on attapulgite, which were marked out by orange arrow, and the Cu_2O-attapulgite nanoparticles were well distributing throughout the sheets of RGO (Fig. 3D).

3.4 Electrochemical behaviour of Cu_2O-attapulgite/RGO/GCE

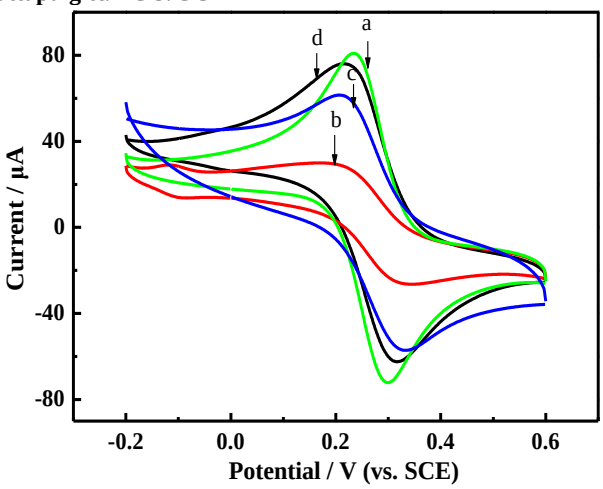

Fig. 4 CVs on bare GCE (a), Cu_2O-attapulgite/GCE (b) and Cu_2O/RGO/GCE (c) and Cu_2O-attapulgite/RGO/GCE (d) in 1.0 mM $K_3Fe(CN)_6$ + 0.10 M KCl solution. Scan rate: 50 mV s^{-1}.

$[Fe(CN)_6]^{3-/4-}$ was usually used as a electrochemical probe to test the electron transfer kinetic between electrodes and the species in solution. Potential difference of anodic and cathodic peaks (ΔE_p) was frequently employed to evaluate electron transfer kinetics[32].

Shown in Fig. 4 were CVs of 1.0 mM $K_3Fe(CN)_6$ in 0.10 M KCl solution on different modified electrodes. ΔE_p of 194 mV on Cu_2O-attapulgite/GCE (Fig. 4b) was larger than that obtained on bare GCE (Fig. 4a), because Cu_2O-attapulgite inhibited to some degree the electron transfer of $[Fe(CN)_6]^{3-/4-}$ to the electrode surface for the poor electro-conductivity of clay[33]. In addition, ΔE_p of $[Fe(CN)_6]^{3-/4-}$ probe on Cu_2O/RGO/GCE was about 136 mV (Fig. 4c), which was smaller than that on Cu_2O-attapulgite/GCE, presumably due to that small amount of Cu_2O nanopartices prevented RGO from agglomerating, so RGO with excellent electro-conductivity provided the necessary conduction pathways, assisting the fast electron transfer between $[Fe(CN)_6]^{3-/4-}$ ions and Cu_2O/RGO/GCE. As expected, the smallest ΔE_p of 107 mV was obtained for $[Fe(CN)_6]^{3-/4-}$ probe on Cu_2O-attapulgite/RGO/GCE (Fig. 4d), which was presumably due to that Cu_2O-attapulgite played a vital role in increasing the electroactive surface area by further reducing the agglomeration of RGO, and the Cu_2O-attapulgite/RGO provided the best conduction pathways[34]. Hence, the well-defined Cu_2O-attapulgite/RGO film on electrode possessed the requisite surface structure and electronic properties to support rapid electron transfer for this particular mechanistically complicated redox system.

3.5 Electrochemical detection of glucose on Cu_2O-attapulgite/RGO/GCE

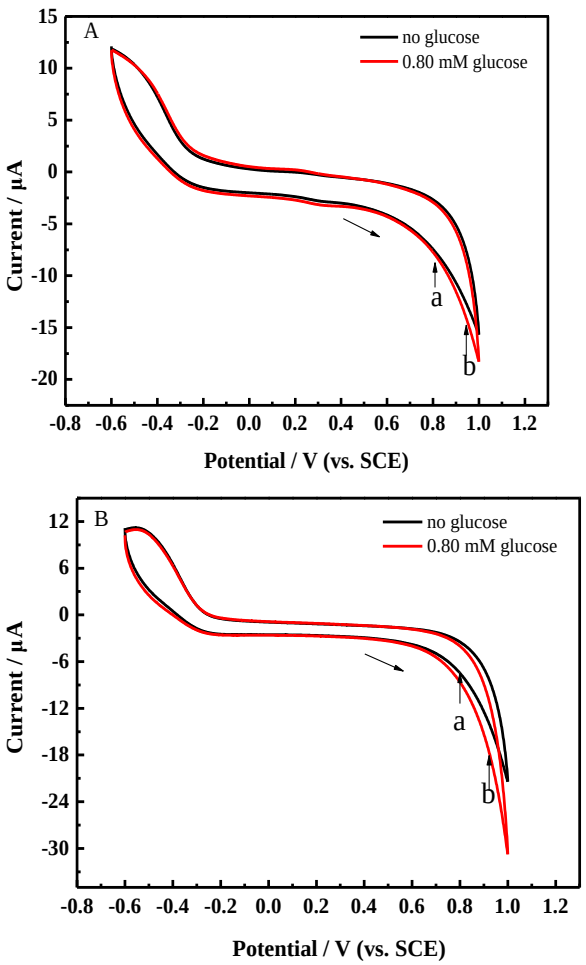

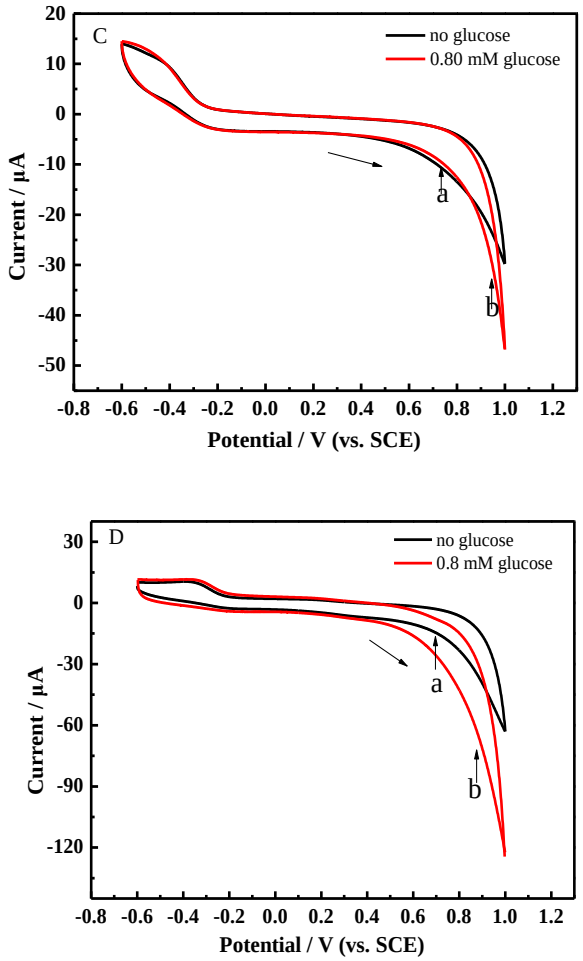

Fig. 5 CVs on bare GCE (A), Cu_2O-attapulgite/GCE (B), RGO/GCE (C) and Cu_2O-attapulgite/RGO/GCE (D) in 0.10 M NaOH solution in the absence (a) and presence (b) of 8.0×10^{-4} M glucose. Scan rate: 50 mV s^{-1}.

To testify the electrochemical properties and sensing applications of the biosensors in glucose detection, the CV responses on different modified electrodes in 0.10 M NaOH with and without 8.0×10^{-4} M glucose were presented in Fig. 5. The CVs on GCE were almost the same when in the presence of glucose or not, indicating that GCE showed no response to glucose oxidation (Fig. 5A). Upon the addition of glucose into electrolyte with a concentration of 8.0×10^{-4} M, increasing anodic current could be detected at about 0.60 V because of the good electrocatalytic activity of as-synthesized Cu_2O-attapulgite towards glucose oxidation (Fig. 5B). As for RGO/GCE, glucose caused a slight increase in the anodic current at the potential above 0.50 V. Excellent electro-conductivity and numerous reaction sites of RGO were the important reasons for its high electrocatalytic performances (Fig. 5C). While for Cu_2O-attapulgite/RGO/GCE, upon the addition of glucose, much higher increase of anodic current and lower starting potential of 0.40 V for glucose oxidation could be obtained, demonstrating that Cu_2O-attapulgite/RGO/GCE exhibited enhanced electrocatalytic activity for glucose oxidation (Fig. 5D). On one hand, it may be ascribed to kinetic effect by the increased electrocatalytic surface area and the improved electron transfer ability of RGO. On the

other hand, Cu_2O-attapulgite/RGO wrapped by RGO nanosheets showed improved electrochemical stability and electrocatalytic activity compared with Cu_2O-attapulgite alone[35]. Such enhanced electrocatalytic performance of Cu_2O-attapulgite/RGO nanocomposites could be ascribed to the synergistic effect between RGO and the loaded Cu_2O-attapulgite nanoparticles, resulting in the high catalytic active sites for glucose oxidation provided by well-distributed Cu_2O nanoparticles and the fast electron transfer channel offered by RGO with large surface area and excellent conductivity.

3.6 Amperometric detection of glucose on Cu_2O-attapulgite/RGO/GCE

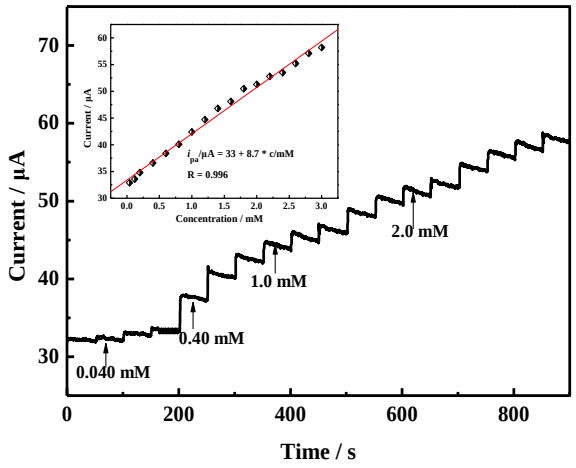

Fig. 6 Current-time plot of glucose with increasing concentrations on Cu_2O-attapulgite/RGO/GCE in 0.10 M NaOH solution. Inset was the linear calibration plot of peak currents versus concentrations. Applied potential: 0.40 V.

Shown in Fig. 6 was amperometric response of glucose on Cu_2O-attapulgite/RGO/GCE obtained by successively adding glucose to a continuously stirred electrochemical cell. Inset was the linear calibration plot of peak currents versus concentrations. Based on the data shown in Fig. 6, it could be ascertained that the oxidation currents of glucose were linear with concentrations. The linear regression equation was calculated as i_{pa} / μA = 33 + 8.7 × c / mM in the range of 4.0 × 10^{-5} M ~ 3.0 × 10^{-3} M (R = 0.996). Based on the signal-to-noise ratio of 3 (S/N = 3), the detection limit was calculated as 2.1 × 10^{-6} M. As prepared Cu_2O-attapulgite/RGO/GCE showed a reasonable sensitivity and a comparatively low detection limit, and the comparison results with other biosensors were shown in Table 1[35-40]. Apparently, the detection limit of Cu_2O-attapulgite/RGO/GCE in this work was higher than those on CuNWs/GTE/ITO and CuO/Ni foam, while lower than the other four glucose biosensors.

Table 1 Performance comparison between Cu_2O-attapulgite/RGO/GCE and other reported glucose sensors

Electrode materials	Linear range (μM)	Detection limit (μM)	References
Cu_2O/GNs	300 ~ 3300	3.3	35
Cu_xO/Cu	0 ~ 4000	49	36
Cu_2O	0 ~ 500	38	37
CuNWs/GTE	5 ~ 6000	1.6	38
CuO/Ni foam	0.5 ~ 3500	0.16	39
CQDs/octahedral Cu_2O	20 ~ 4300	8.4	40
Cu_2O-attapulgite/RGO	4.0 ~ 3000	2.1	this work

3.7 Effect of interferences on analytical response

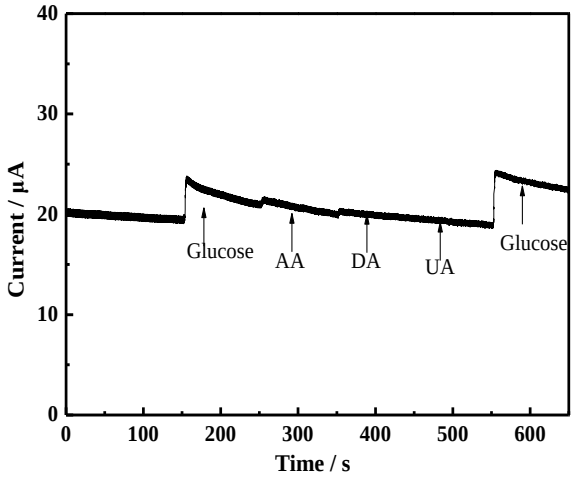

Fig. 7 Interference test of Cu_2O-attapulgite/RGO/GCE in 0.10 M NaOH at an applied potential of 0.40 V with 0.30 mM glucose and other interferents as indicated.

One of the important analytical factors for an amperometric biosensor was its ability to discriminate the interfering species having electroactivities similar to target analyte. The selectivity of biosensor was investigated using DA, AA and UA as interferents normally co-existing with glucose in biological sample which could be easily oxidized and consequently obtained overlapped responses to interfere with the detection of glucose. Considering that the concentration of glucose in human blood was about 30 times of interfering species, the interference experiment was carried out by successive addition of 0.30 mM glucose and 0.010 mM AA, DA, UA as interfering species in 0.10 M NaOH in the present work. The measured effects of different interferents along with glucose at 0.40 V were shown in Fig. 7. For all the interfering species, Cu_2O-attapulgite/RGO/GCE showed no any significant responses, indicating that Cu_2O-attapulgite/RGO/GCE was highly specific and sensitive to glucose even in the presence of several interfering species normally found in biological samples.

3.8 Stability and reproducibility

Stability and reproducibility were important properties to evaluate the performance of modified electrodes. Thus, stability of Cu_2O-attapulgite/RGO/GCE was evaluated by measuring the decrease of current response to 1.0 mM glucose over two weeks. The electrochemical sensor exhibited no obvious decrease in current response and maintained about 93% of its initial response. Five measurements for 1.0 mM glucose on Cu_2O-attapulgite/RGO/GCE were investigated and the RSD was 2.8%,

confirming that Cu_2O-attapulgite/RGO/GCE had high reproducibility. The results above showed that as prepared Cu_2O-attapulgite/RGO/GCE presented long-time stability and satisfactory reproducibility for the detection of glucose.

4 Conclusions

In this work, a novel one-pot hydrothermal approach was first proposed to prepare Cu_2O-attapulgite/RGO, which was used for the construction of glucose biosensor. It was found that the integrated composite combined the merits of each component and yielded enhanced properties via synergistic effect, and a linear concentration range of 4.0×10^{-5} M ~ 3.0×10^{-3} M with a detection limit of 2.1×10^{-6} M was achieved. We believed that such a facile method herein would be of great significance for the construction of non-enzyme biosensor for the detection of glucose in a convenient way.

Acknowledgements

We are grateful to anonymous reviewers for their helpful and insightful comments. This work was supported by the Open Project of State Key Laboratory Cultivation Base for Nonmetal Composites and Functional Materials (11zxfk26). Also we are grateful for the help of Analytical and Testing Center of Southwest University of Science and Technology.

Notes and references

a State Key Laboratory Cultivation Base for Nonmetal Composites and Functional Materials, School of Materials Science and Engineering, Southwest University of Science and Technology, Mianyang 621010, P. R. China. Fax: 86-816-6089371; E-mail: heping@swust.edu.cn. Tel.: 86-816-6089371.

b Center of Analytical Test, Southwest University of Science and Technology, Mianyang 621010, Sichuan, P. R. China

1 K. M. E. Khatib and R. M. A. Hameed, *Biosens. Bioelectron.*, 2011, **26**, 3542.
2 M. Labib, M. Hedstrom, M. Amin and B. Mattiasson, *Anal. Chim. Acta*, 2010, **659**, 194.
3 Z. C. Xing, J. Q. Tian, A. M. Asiri, A. H. Qusti, A. O. Al-Youbi and X. P. Sun, *Biosens. Bioelectron.*, 2014, **52**, 452.
4 T. G. S. Babu and T. Ramachandran, *Electrochim. Acta*, 2010, **55**, 1612.
5 J. Wang, *Chem. Rev.*, 2008, **108**, 814.
6 L. C. Jiang and W. D. Zhang, *Biosens. Bioelectron.*, 2010, **25**, 1402.
7 C. Y. Ko, J. H. Huang, S. Raina and W. P. Kang, *Analyst*, 2013, **138**, 3201.
8 S. Z. Bas, *Anal. Methods*, 2014, **6**, 7752.
9 J. H. Wang, W. G. Bao and L. J. Zhang, *Anal. Methods*, 2012, **4**, 4009.
10 L. C. Chen, Mater. *Sci. Semicond. Process.*, 2013, **16**, 1172.
11 X. Y. Shen, S. Chen, D. B. Mu, B. R. Wu and F. Wu, *J. Power Sources*, 2013, **238**, 173.
12 M. Y. Wang, J. R. Huang, Z. W. Tong, W. H. Li and J. Chen, *J. Alloys Compd.*, 2013, **568**, 26.
13 S. Z. Deng, V. Tjoa, H. M. Fan, H. R. Tan, D. C. Sayle, M. Olivo, S. Mhaisalkar, J. Wei and C. H. Sow, *J. Am. Chem. Soc.*, 2012, **134**, 4905.
14 L. C. Wang and M. Tao, *Electrochem. Solid-State Lett.*, 2007, **10**, H248.
15 S. F. Wu, T. M. Liu, W. Zeng, S. X. Cao, K. G. Pan, S. Y. Li, Y. S. Yan, J. J. He, B. Miao and X. H. Peng, *J. Mater. Sci. - Mater. Electron.*, 2014, **25**, 974.
16 L. S. Xu, X. H. Chen, Y. R. Wu, C. S. Chen, W. H. Li, W. Y. Pan and Y. G. Wang, *Nanotechnology*, 2006, **17**, 1501.
17 J. H. Huang, X. G. Wang, Q. Z. Jin, Y. F. Liu and Y. Wang, *J. Environ. Manage.*, 2007, **84**, 229.
18 S. C. Mu, M. Pan and R. Z. Yuan, *Mater. Sci. Forum*, 2005, **475–479**, 2441.
19 S. D. Miao, Z. M. Liu, Z. F. Zhang, B. X. Han, Z. J. Miao, K. L. Ding and G. M. An, *J. Phys. Chem. C*, 2007, **111**, 2185.
20 S. S. Zhang, P. He, W. Lei and G. L. Zhang, *J. Electroanal. Chem.*, 2014, **724**, 29.
21 X. M. Feng, R. M. Li, Y. W. Ma, R. F. Chen, N. E. Shi, Q. L. Fan and W. Huang, *Adv. Funct. Mater.*, 2011, **21**, 2989.
22 X. Y. Jiang, Y. Q. Chai, R. Yuan, Y. L. Cao, Y. F. Chen, H. J. Wang and X. X. Gan, *Anal. Chim. Acta*, 2013, **783**, 49.
23 Z. J. Fan, Q. Q. Lin, P. W. Gong, B. Liu, J. Q. Wang and S. R.Yang, *Electrochim. Acta*, 2015, **151**, 186.
24 W. S. Hummers, *J. Am. Chem. Soc.*, 1958, **80**, 1339.
25 A. C. Ferrari and J. Robertson, *Phys. Rev. B*, 2000, **61**, 14095.
26 V. Chandra, J. Park, Y. Chun, J. W. Lee, I. C. Hwang, and K. S. Kim, *ACS Nano*, 2010, **4**, 3979.
27 A. Gupta, G. Chen, P. Joshi, S. Tadigaapa and P. C. Eklund, *Nano Lett.*, 2006, **6**, 2667.
28 L. H. Wang and J. Sheng, *Polymer*, 2005, **24**, 6243.
29 M. Salavati-Niasari and F. Davar, *Mater. Lett.*, 2009, **63**, 441.
30 Q. Jiang, Z. Y. Wu, Y. M. Wang, Y. Cao, C. F. Zhou and J. H. Zhu, , *J. Mater. Chem.*, 2006, **16**, 1536.
31 J. Luo, S. S. Jiang, H. Y. Zhang, J. Q. Jiang and X. Y. Liu, *Anal. Chim. Acta*, 2012, **709**, 47.
32 J. B. Jia, B. Q. Wang, A. G. Wu, G. J. Cheng, Z. Li and S. J. Dong, *Anal. Chem.*, 2002, **74**, 2217.
33 Y. S. Liu, P. Liu and Z. X. Su, *Synth. Met.*, 2007, **157**, 585.
34 P. He, W. Wang, L. C. Du, F. Q. Dong, Y. Q. Deng and T. H. Zhang, *Anal. Chim. Acta*, 2012, **739**, 25.
35 M. M. Liu, R. Liu and W. Chen, *Biosens. Bioelectron.*, 2013, 45. 206.
36 C. L. Li, Y. Su, S. W. Zhang, X. Y. Lv, H. L Xia and Y. J. Wang, *Biosens. Bioelectron.*, 2010, **26**, 903.
37 S. Felix, P. Kollu, B. P C Raghupathy, S. K. Jeong and A. N. Grace, *J. Chem. Sci.*, 2014, **126**, 25.
38 Z. J. Fan, B. Liu, X. H. Liu, Z. P. Li, H. G. Wang, S. R. Yang and J. Q. Wang, *Electrochim. Acta*, 2013, **109**, 602.
39 Z. J. Fan, B. Liu, Z. P. Li, L. M. Ma, J. Q. Wang and S. R.Yang, *RSC Adv.*, 2014, **4**, 23319.
40 Y. C. Li, Y. M. Zhong, Y. Y. Zhang, W. Weng, S. X. Li, *Sens. Actuat. B: Chem.*, 2015, **206**, 735.